Dynamic shear modulus and damping of compacted silty sand via suction-controlled resonant column testing

Propriétés dynamiques d'un sable limoneux par des tests en colonne de résonance sous aspiration contrôlée.

Hoyos L.R., Cruz J.A., Puppala A.J., Douglas W.A., Suescún E.A.
University of Texas at Arlington, Arlington, Texas 76019, USA

ABSTRACT: Dynamic properties of unsaturated soils, particularly shear modulus and material damping, play a fundamental role in the analysis/design of critical geotechnical infrastructure resting on unsaturated ground, or made of compacted unsaturated soils, when subjected to static and dynamic loads. This paper introduces a proximitor-based resonant column device with self-contained bender elements suitable for testing soils under controlled-suction conditions via the axis-translation technique. A series of suction-controlled resonant column and bender element tests were conducted on several statically compacted samples of silty sand under net stresses and suction states ranging from 50-400 kPa. Particular attention was devoted to the influence of suction over the frequency response curves and cyclic hysteretic stress-strain loops. The results confirm the influence exerted by the stress/suction history experienced by the soil, in terms of dynamic shear modulus and damping.

RÉSUMÉ: Les propriétés dynamiques des sols non saturés, en particulier le module de cisaillement dynamique et l'amortissement, jouent un rôle clé dans l'analyse et la conception de l'infrastructure civile sous des charges statiques ou dynamiques. Dans cet article, un appareil de colonne de résonance a été utilisé pour tester des échantillons de sol non saturé dans des conditions contrôlées d'aspiration. Les essais en colonne de résonance ont été effectués sur des échantillons de sable limoneux compacté statiquement, sous des succions de 50-400 kPa. Les résultats confirment l'influence des chemins de contrainte et des succions sur les échantillons de sol, en termes de module dynamique de cisaillement et d'amortissement.

KEYWORDS: unsaturated soil, matric suction, axis-translation, resonant column test, shear modulus, damping, cyclic hysteretic loop.

1 INTRODUCTION

Dynamic properties of unsaturated soils, particularly shear modulus and material damping, play a fundamental role in the analysis/design of critical geotechnical infrastructure resting on unsaturated ground, or made of compacted unsaturated soils, when subjected to static or dynamic loads. Most conventional soil testing techniques, however, cannot capture this very small-strain behavior and thereby considerably underestimate the true soil stiffness. Several efforts have been reported since the early 1980's to study the effects of capillarity and saturation on small-strain stiffness of unsaturated soils via resonant column (RC) or bender element (BE) testing, including Brull (1980), Wu et al. (1984), Qian et al. (1991), Marinho et al. (1995), Picornell and Nazarian (1998), Cabarkapa et al. (1998), Cho and Santamarina (2001), Mancuso et al. (2002), Inci et al. (2003), Kim et al. (2003), Mendoza et al. (2005), Cabarkapa and Cuccovillo (2006), Vassallo et al. (2006), Sawangsuriya et al. (2008, 2009), Ng et al. (2009), and Khosravi et al. (2010).

The BE technique has proved a feasible way to investigate unsaturated soil stiffness at very small shear strain amplitudes. However, there is a great need for assessing the suitability of this technique, particularly for unsaturated soils, as compared to more fully-standardized procedures such as the resonant column and simple shear test methods.

This paper introduces a suction-controlled proximitor-based resonant column apparatus which features self-contained BEs for the simultaneous testing of soils under both techniques. Particular attention is devoted to the influence of suction over the frequency response curves and cyclic hysteretic stress-strain loops. The results highlight the critical influence exerted by the stress/suction history experienced by the soil in terms of both dynamic shear modulus and damping.

2 RC/BE DEVICE: MAIN FEATURES

The model THS-100 resonant column cell features a reinforced acrylic chamber of 1000 kPa confining pressure capacity. The bottom pedestal, for samples of 70-mm diameter, features a full set of HAEV (5-bar) ceramic disks, as well as one BE crystal (receiver) for shear-wave velocity readings: Figure 1(a). The top cap features a full set of coarse porous stones, for uniform pore-air pressure application/control, and also one BE transmitter. An electrical servo motor actuator is used for the application of torsional loads with +/– 2 3.3 kN-m (peak) capacity, and 300-Hz frequency range.

The input torque is measured in pfs (percent of full scale) units, with 100 pfs equivalent to a 10 kN-m torque. Mounted on an internal floating frame, thus allowing for large vertical deformations, the actuator includes a servo amplifier for closed-loop control of torsional loads, and one proximitor mounting acting as the internal angular displacement transducer: Figure 1(b). A model PCP-15U pressure panel is used for direct control of pore-air pressure u_a through the top cap, with dual pressure regulators/gauges for precise measurement/control of matric suction, $s = u_a$ ($u_w = 0$).

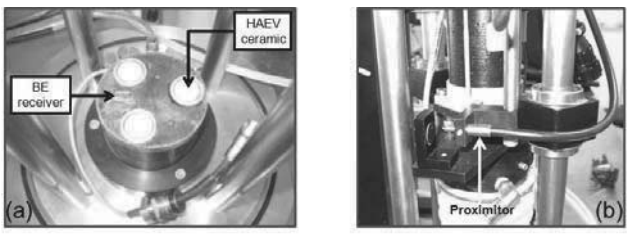

Figure 1. THS-100 resonant column cell with self-contained BEs.

3 TEST SOIL AND PERFORMANCE VERIFICATION

The soil material used in this work classifies as silty sand (SM) according to the USCS: 70% sand and 30% silt. The coarse fraction has particle sizes between 0.5-1.2 mm. The passing No. 40 sieve fraction has liquid limit, LL = 26.4%, and plastic limit, PL = 22.2%. Samples were statically compacted into a 70-mm diameter, 130-mm height, compaction split mold via a triaxial loading frame. Each sample was prepared in three lifts, at a constant displacement rate of 1.0 mm/min, to a target void ratio, e = 1.0, and dry unit weight, γ_d = 13.13 kN/m^3. The initial water content of 26% corresponds to an average degree of saturation of 72% and initial matric suction of 20 kPa, according to the soil-water retention curve (Hoyos et al. 2011).

Calibration of the proximitor-based RC device was first accomplished by conducting resonant column tests on a 9.5 mm (0.375 in) diameter, stainless aluminum rod, which also yields the polar moment of inertia of the entire drive system. The test yielded expected values for torsional stiffness of the aluminum rod, k = 26.4 GPa, and polar moment of inertia of the drive system, I_o = 737.8 kg-mm^2. Performance verification testing was then carried out through a comparative analysis of results from proximitor-based RC tests and accelerometer-based RC tests (ASTM 1993) on identically prepared samples of SM soil.

Figure 2(a) shows a full set of frequency response curves obtained from compacted SM soil in the accelerometer-based RC device. The specimen was subject to different input-voltage amplitudes ranging from 0.25 to 5 Volts, thus generating a family of curves with different resonant frequencies and peak accelerometer outputs, from which shear modulus G and shear strain amplitude γ can be calculated. All tests were performed under constant 40 psi confinement. Soil softening (degradation) is manifested by the so-called backbone curve. Likewise, Figure 2(b) shows a full set of frequency response curves obtained from an identically prepared sample of SM soil tested in the proximitor-based device. In this case, however, the specimen was subject to different input-torque magnitudes ranging from 1 pfs (0.1 kN-m) to 10 pfs (1 kN-m). Peak shear strain fractions γ (cm/cm) can be readily assessed from each test. All tests were also performed under a constant 40 psi confinement.

Results show that a 1-pfs input torque in the proximitor-based apparatus induces a similar response as a 0.25-Volt input signal in the accelerometer-based apparatus, which is typically used to ensure shear strain levels below a threshold limit γ_{th}. It can also be observed that a 10-pfs input torque induces a higher degree of soil softening than the maximum 5-Volt input signal in the accelerometer-based device. The scope of the present work, however, is limited to linear (low-amplitude or small-strain) stiffness response of unsaturated soils; therefore, a 1-pfs input torque (0.1 kN-m) was adopted for all subsequent suction-controlled tests performed in the proximitor-based RC device, as described in the following section.

4 RC/BE TEST PROCEDURES AND SOIL RESPONSE

A series of RC and BE tests were simultaneously conducted on identically prepared samples of SM soil. Each sample was tested under constant matric suction, s = 50, 100, 200, or 400 kPa, induced via axis-translation technique; and four different net confining pressures, $(p - u_a)$ = 50, 100, 200, and 400 kPa. The soil was first isotropically compressed to a target confining pressure, p = 50 kPa. Pore-air pressure u_a was then gradually increased (soil drying) to the pre-established value of suction, while the net confining pressure was kept constant at 50 kPa by simultaneous and equal increases of the external confinement.

Pore-air pressure u_a was maintained constant until no further change in water volume from within the soil (less than 0.035 ml/day) was observed, at which point pore-fluids equalization was considered complete. A 36-hr equalization time (1.5 days) was found suitable for all suction states. Equalization stage was finally followed by a constant-suction ramped consolidation to the target values of net confining pressure. All RC tests were conducted by sweeping the entire input-torque frequency scale until obtaining a thorough frequency response curve, typically between 50 and 250 Hz. The peak torsional vibration was then completely cut off to record the free-vibration decay curve.

Figure 3(a) shows a family of typical frequency response curves obtained from suction-controlled RC tests on SM soil under constant matric suction, s = 50 kPa, and net confining pressures, $(p - u_a)$ = 50, 100, 200, and 400 kPa. Likewise, Figure 3(b) shows typical curves under constant matric suction, s = 200 kPa. It can be readily observed the critical influence that suction has on soil response under resonance, with a significant rightward shift of all curves for higher suction state, s = 200 kPa. This can be directly attributed to the expected increase in effective stress and, hence, rigidity (stiffness) of soil skeleton at higher suctions. The level of net confinement, however, has a more pronounced effect than matric suction. It can also be observed that the half-power points, that is, frequencies on each side of the frequency response curves corresponding to a shear strain of 0.707(γ_{max}), become less apparent as suction increases, i.e., the frequency response is less symmetric about the resonant frequency. Hence, the assessment of material damping using the half-power bandwidth method becomes less reliable at higher suction states.

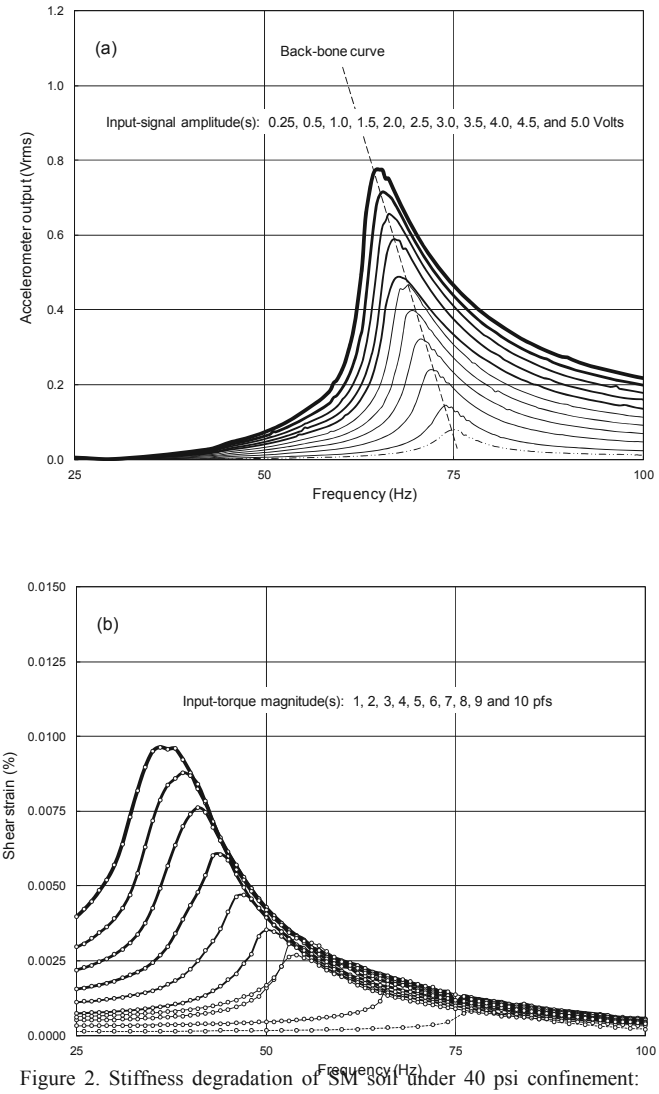

Figure 2. Stiffness degradation of SM soil under 40 psi confinement: (a) accelerometer RC device; and (b) proximitor RC device.

5 DYNAMIC SHEAR MODULUS AND DAMPING

Figure 4 shows the variation of small-strain shear modulus G_{max} (from both RC and BE tests) with net confining pressure, and for different suction values. The trends confirm those shown in Figure 3: suction is observed to have a significant influence on soil stiffness, though not as pronounced as that of net confining pressure. The BE technique yields G_{max} values reasonably close to those obtained via resonant column testing. Solid lines in Figure 4 represent best-fit power regression functions of the form, $G_{max} = A(p - u_a)^B$. Constant A represents the value of G_{max} (MPa) at net confining pressure, $(p - u_a) = 1$ kPa; while constant B is the slope of the best-fit curve, which represents how susceptible soil stiffness is to changes in net confinement $(p - u_a)$.

During bender element testing, the first arrival of shear-wave was taken as the point of zero crossing after the first inflection of the received signal, which corresponds to the first arrival of the shear-wave based upon experimental and numerical studies (Lee and Santamarina 2005). The travel distance is taken as the tip-to-tip distance L between bender elements, hence the shear-wave velocity is computed as $V_s = L/t$, where t = travel time. Knowing V_s and the total mass (bulk) density of the specimen ρ, the small-strain shear modulus can be determined as $G = \rho(V_s)^2$.

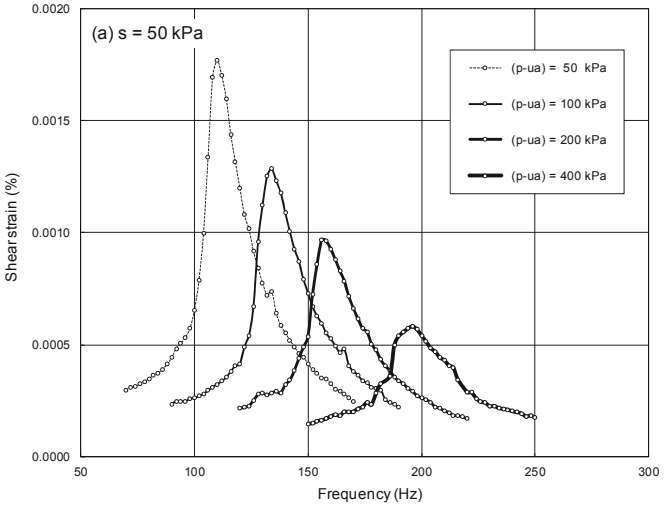

Figure 3. Frequency response curves from SM soil at different net confinement and suction states: (a) s = 50 kPa; and (b) s = 200 kPa.

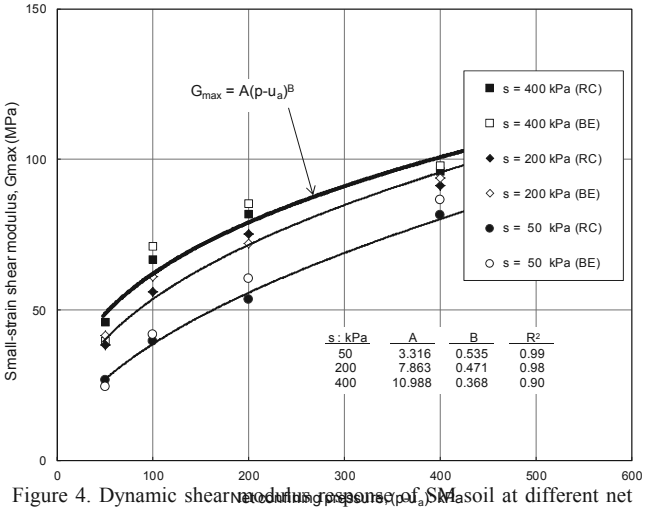

Figure 4. Dynamic shear modulus response of SM soil at different net confinements and matric suction states.

Figure 5 shows the change in small-strain damping ratio D_{min} (from RC tests) with matric suction, for different net confining pressures. Damping is calculated from logarithmic decay curves using: $D_{min} = (1/2\pi n)\log_e(Z_o/Z_n)$; where, Z_o = peak amplitude of the first free-vibration cycle, and Z_n = peak amplitude of the nth cycle. The trends confirm those in Figure 3, with lower damping (higher stiffness) at higher matric suctions. In general, material damping tends to be overestimated by the half-power bandwidth method: $D_{min} = (1/2)(f_2 - f_1)/f_r$; where f_r = resonant frequency.

The main focus of the present work has been on small-strain stiffness of compacted silty sand. The cyclic behavior of soils, however, is nonlinear and hysteretic; consequently, the shear modulus and material damping are heavily strain dependent. Figure 6 shows the cyclic hysteretic stress-strain loops from two SM soil samples subjected to a cyclic 10-pfs input torque (1 kN-m) at matric suctions, s = 50 kPa (thinner trace) and s = 200 kPa (thicker trace), respectively; both under the same net confining pressure, $(p - u_a) = 200$ kPa. Equivalent viscous damping could also be evaluated from the area enclosed by the cyclic hysteretic loops. Therefore, the loops further substantiate the trends shown in Figure 5, with smaller areas enclosed by the cyclic hysteretic loops, and lower shear strains induced by the same cyclic shear stress, with increasing matric suction.

6 CONCLUDING REMARKS

Suction-controlled resonant column tests on compacted SM soil shows that the newly implemented proximitor-based RC device is suitable for testing soils under controlled suction states via axis-translation technique. Test results underscore the influence of soil suction over the frequency response curves, logarithmic decay curves, cyclic hysteretic stress-strain loops, and the small-strain stiffness properties of compacted SM soil. Lower material damping (higher stiffness) is observed at higher suction states. In general, material damping tends to be overestimated by the half-power bandwidth method. Simultaneous suction-controlled bender element tests produced G_{max} values reasonably close to those from resonant column tests.

The general trends observed in this research effort are similar to those previously reported for a more limited range of test variables (e.g., Kim et al. 2003, Sawangsuriya et al. 2009, Ng et al. 2009). The time frame and scope of the present work did not contemplate investigating the effects of initial void ratio, stress history, hydraulic hysteresis, or the impact of net normal stress and/or suction history on the normalized G/G_{max} and D/D_{min} response of SM soil. The authors are currently embarked on a more thorough research effort to gain further insight into all these dynamic aspects of unsaturated soil behavior, including

RC/BE testing at matric suction states near the air-entry value of the test soil.

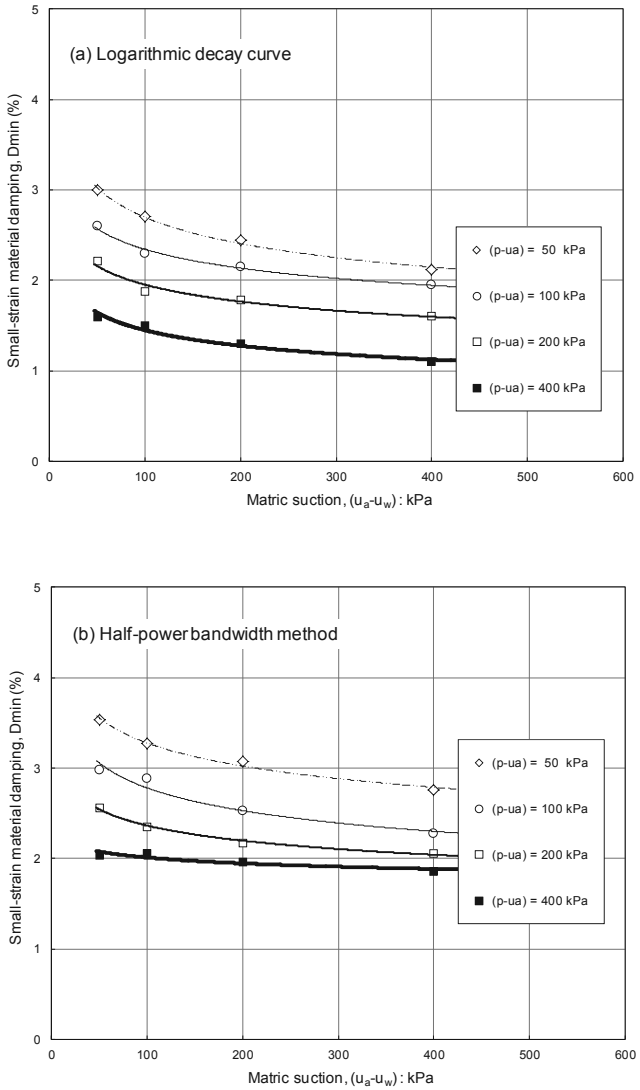

Figure 5. Damping response of SM soil at different net confinements and matric suction states.

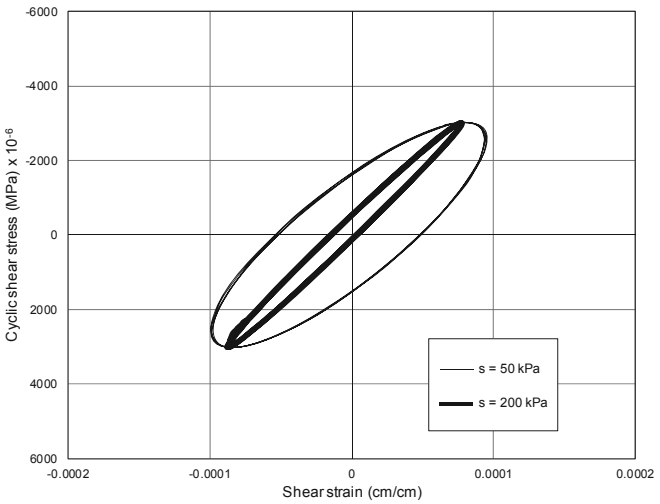

Figure 6. Cyclic hysteretic shear stress vs. shear strain loops from SM soil samples subjected to a cyclic 10-pfs input torque (1 kN-m).

7 REFERENCES

ASTM 1993. Test methods for modulus and damping of soils by the resonant column method. *Standard D 4015-92*, American Society for Testing and Materials, Philadelphia, PA, 581-593.

Brull A. 1980. Caracteristiques mécaniques des sols de fondation de chaussées en fonction de leur état d'humidité et de compacité. *Proceedings of International Conference on Soil Compaction*, Paris, France, vol. 1, 113-118.

Cabarkapa Z. and Cuccovillo T. 2006. Automated triaxial apparatus for testing unsaturated soils. *Geotechnical Testing Journal*, ASTM, 29(1), 1-9.

Cabarkapa Z., Cuccovillo T. and Gunn M. 1998. A new triaxial apparatus for testing unsaturated soils. *Proceedings of Second International Conference on Unsaturated Soils*, Beijing, China, vol. 2, 194-195.

Cho G.C. and Santamarina J.C. 2001. Unsaturated particulate materials: Particle-level studies. *J. of Geotechnical and Geoenvironmental Engineering*, ASCE, 127(1), 84-96.

Hoyos L.R., Suescún E.A. and Puppala A.J. 2011. Small-strain stiffness of unsaturated soils using a suction-controlled resonant column device with bender elements. *Advances in Geotechnical Engineering*, GSP 211, Geo-Institute of ASCE, Proceedings of Geo-Frontiers 2011, March 13-16, 2011, Dallas, Texas, Eds: J. Han and D.E. Alzamora, 4313-4322.

Inci G., Yesiller N. and Kagawa T. 2003. Experimental investigation of dynamic response of compacted clayey soils. *Geotechnical Testing Journal*, ASTM, 26(2), 125-141.

Kim D.S., Seo W.S. and Kim M.J. 2003. Deformation characteristics of soils with variations of capillary pressure and water content. *Soils and Foundations*, 43(4), 71-79.

Khosravi A., Ghayoomi M., McCartney J. and Ko H.Y. (2010). Impact of effective stress on the dynamic shear modulus of unsaturated sand. *Advances in Analysis, Modeling & Design*, GSP 199, Geo-Institute of ASCE, Proceedings of GeoFlorida 2010, February 20-24, 2010, West Palm Beach, Florida, Eds: D. Fratta, A.J. Puppala, and B. Muhunthan, 410-49.

Lee J.-S. and Santamarina J.C. 2005. Bender elements: performance and signal interpretation. *J. of Geotechnical and Geoenvironmental Engineering*, ASCE, 131(9), 1063-1070.

Mancuso C., Vassallo R. and d'Onofrio A. 2002. Small strain behavior of a silty sand in controlled-suction resonant column-torsional shear tests. *Canadian Geotechnical Journal*, 39, 22-31.

Marinho F.A.M., Chandler R.J. and Crilly M.S. 1995. Stiffness measurements on unsaturated high plasticity clay using bender elements. *Proceedings of First International Conference on Unsaturated Soils*, September 6-8, 1995, Paris, France, Eds: E.E. Alonso and P. Delage, vol. 2, 535-539.

Mendoza C.E., Colmenares J.E. and Merchán V.E. 2005. Stiffness of an unsaturated compacted clayey soil at very small strains. *Advanced Experimental Unsaturated Soil Mechanics*, Balkema, International Symposium on Advanced Experimental Unsaturated Soil Mechanics, June 27-29, 2005, Trento, Italy, Eds: A. Tarantino, E. Romero, and Y.J. Cui, 199-204.

Ng C.W.W., Xu J. and Yung S.Y. 2009. Effects of imbibition-drainage and stress ratio on anisotropic stiffness of an unsaturated soil at very small strains. *Canadian Geotechnical Journal*, 46, 1062-1076.

Picornell M. and Nazarian S. 1998. Effects of soil suction on low-strain shear modulus of soils. *Proceedings of Second International Conference on Unsaturated Soils*, August 27-30, 1998, Beijing, China, vol. 1, 102-107.

Qian X., Gray D.H. and Woods R.D. 1991. Resonant column tests on partially saturated sands. *Geotechnical Testing Journal*, ASTM, 14(3), 266-275.

Sawangsuriya A., Edil T.B. and Bosscher P.J. 2009. Modulus-suction-moisture relationship for compacted soils in postcompaction state. *J. of Geotechnical and Geoenvironmental Engineering*, ASCE, 135(10), 1390-1403.

Sawangsuriya A., Edil T.B. and Bosscher P.J. 2008. Modulus-suction-moisture relationship for compacted soils. *Canadian Geotechnical Journal*, 45, 973-983.

Vassallo R., Mancuso C. and Vinale F. 2006. Effects of net stress and suction history on small strain stiffness of a compacted clayey silt. *Canadian Geotechnical Journal*, 44, 447-462.

Wu S., Gray D.H. and Richart F.E. Jr. 1984. Capillary effects on dynamic modulus of sands and silts. *Journal of Geotechnical Engineering*, ASCE, 110(9), 1188-1203.